ELMs and disruptions in ITER : Expected Energy Fluxes on Plasma-Facing Components from Multi-machine Experimental Extrapolations and Consequences for ITER Operation

A. Loarte 1), G. Saibene 1), R. Sartori 1), D. Campbell 1), V. Riccardo 2), P. Andrew 2), G.F. Matthews 2), J. Paley 2), W. Fundamenski 2), T. Eich 3), A. Herrmann 3), G. Pautasso 3), A. Kirk 2), G. Counsell 2), G. Federici 4), G. Strohmayer 4), M. Merola 4), K.H. Finken 5), J. Linke 5), G. Maddaluno 6), D. Whyte 7,8), A. Leonard 8), M. Fenstermacher 8), R.A. Pitts 9), I. Landman 10), B. Bazylev 10), S. Pestchanyi 10), A. Zhitlukhin 11), V. Podkovyrov 11) , N. Klimov 11), V. Safronov 11), M. Becoulet 12), B. Kuteev 13), V. Koidan 13), L. Khimchenko 13)

1) EFDA Close Support Unit Garching, Boltmannstr.2, D-85748 Garching bei München, Germany
2) Euratom-UKAEA Fusion Association, Culham Science Centre, Abingdon OX11 3EA, United Kingdom
3) Association Euratom-Max-Planck Institut für Plasmaphysik, Boltmannstr.2, D-85748 Garching bei München, Germany
4) ITER International Team, Garching Working Site, Boltmannstr.2, D-85748 Garching bei München, Germany
5) Association EURATOM - Forschungszentrum Jülich GmbH, D-52425 Jülich, Germany
6) Association Euratom-ENEA Frascati, via Enrico Fermi 45, 00044 Frascati, Italy
7) Dept. Engineering Physics, University of Wisconsin-Madison, 1500 Engineering Dr., Madison, WI 53706, USA
8) DIII-D National Fusion Facility, P.O. Box 85608, San Diego, CA 92186, USA
9) Centre de Recherches en Physique des Plasmas (CRPP), École Polytechnique Fédérale de Lausanne, Association EURATOM – Conféderation Suisse, 1015 Lausanne, Switzerland
10) Forschungszentrum Karlsruhe, IHM, P.O. Box 3640, 76021 Karlsruhe, Germany
11) SRC RF TRINITI, Troitsk, 142190, Moscow Region, Russia
12) Association Euratom-CEA, CEA/DSM/DRFC, CEA Cadarache, F-13108 St. Paul-lez-Durance, France
13) Nuclear Fusion Institute ,RRC "Kurchatov Institute", Kurchatov sq. 1, 123182, Moscow, Russia

e-mail contact of main author: Alberto.Loarte@efda.org

Abstract. New experimental results on transient loads during ELMs and disruptions in present tokamak devices and their effects on plasma facing materials are described and used to carry out a physics-based extrapolation of the expected loads in ITER reference operating conditions and consequences for the operation of the device. In particular, the achievement of convective Type I ELMs in ITER-like plasma conditions seems to open a way to achieve transient loads which may be compatible with an acceptable erosion lifetime of plasma facing components (PFCs) in ITER. This is reinforced by calculations of the expected erosion lifetime, under these load conditions, which take into account a realistic temporal dependence of the power fluxes on plasma facing components during ELMs and disruptions. On the other hand, the non-ideal behaviour of plasma facing materials seen in dedicated experiments in plasma guns (W cracking and CFC enhanced PAN fibre erosion) may impose additional constraints to ITER operations well below those evaluated on the basis of average material properties.

1. Introduction

Operation of ITER in high fusion gain regimes ($Q_{DT} \geq 10$) requires high density plasmas ($<n_e> \geq 10^{20}$ m^{-3}) with large plasma energy ($W_{th} \geq 320$ MJ), which are achievable in ITER on the basis of scalings from Type I ELMy H-mode discharges in present experimental devices or could be achieved with degraded Type III ELMy H-mode confinement, albeit at larger plasma current and reduced fusion power [1]. A characteristic feature of the ITER Type I ELMy H-mode operating regime is the transient release of energy from the confined plasma onto plasma facing components (PFCs) by Type I ELMs, which in ITER can contribute significantly to the overall erosion rate and lifetime of these

components [2]. Similarly, the transient power fluxes to which PFCs are subject during disruptions can affect significantly their lifetime [3]. This is an issue not intrinsically linked to ELMy H-mode operation but to ITER high fusion power regimes in general and, as such, directly correlated with the achievement of ITER goals and not specific to the final reference regime in which these will be reached.

In the last years, significant progress in the characterisation of the ELM and disruption transient loads in most divertor tokamak experiments has taken place. This has allowed an improved understanding of the physical processes that determine the loss of energy from the main plasma to the PFCs mainly through the measurement capabilities specific to every device and by the development of models to reproduce them. These measurements have provided a physics-based framework on which the expected energy loads on ITER PFCs can be estimated by a combination of physics-based empirical scalings and models applied to the foreseen ITER core and pedestal plasmas.

In parallel with the research on transient loads in tokamaks, significant progress in the experimental characterisation and modelling of the expected PFC material damage under transient loads in ITER has taken place. This research has allowed an improved understanding of the material damage processes for ITER-like ELM and disruption loads for the real materials (CFC and W) /geometries (castellated) of the divertor targets in ITER beyond the initial estimates of divertor target erosion under these loads based on the physical properties of these materials [4, 5].

This paper describes the basis for the present evaluation of the magnitude and the spatial and temporal characteristics of the transient loads on plasma facing components in ITER during Type I ELMs and disruptions and discusses the implications of such loads on the lifetime of ITER's PFCs and on the operation of the device.

2. Power fluxes at the ITER plasma edge during Type I ELMs

The energy loss from the main plasma during Type I ELMs (ΔW_{ELM}) in present experiments is caused by the collapse of the plasma temperature (ΔT_{ELM}, leading to conductive losses) and density (Δn_{ELM}, leading to convective losses) in a region extending up to (~ 0.8 a), where a is the minor radius of the plasma. Type I ELMs with small (normalised to the pedestal energy $W_{ped} = 3$ $n_{e,ped} T_{e,ped} V_{plasma}$) energy losses ($\Delta W_{ELM}/W_{ped} < 0.10$) are associated with small ΔT_{ELM} (typically $\Delta T_{ELM} < 0.2$) and, thus, with the dominance of convection for the transport of energy from the confined plasma onto open field lines which was noted for DIII-D [6] and JET [7]. Fig.1 illustrates this "universal" correlation between the size of ΔW_{ELM} and the change of pedestal temperature at the ELM for a database including data for a large range of plasma conditions at DIII-D [6], JET [7], JT-60U [8] and ASDEX-Upgrade [9]. The spread of the data in this figure is associated with the various diagnostics used for the determination of the ELM temperature (ECE and Thomson scattering) and energy loss (from diamagnetic and kinetic measurements) in the different experimental devices besides variations of the ELM affected area and convective losses with magnetic configurations, etc. This empirical correlation indicates that the route towards small Type I ELM energy losses in ITER goes through the achievement of convective ELMs for those conditions expected at the ITER pedestal plasma, namely high density (normalised to the Greenwald limit) and low collisionality conditions. In most experiments for "standard" operation conditions the achievement of small "convective" ELMs is associated with high density/collisionality operation [6]. More recent experiments at JET [7] and JT-60U [8] have shown that convective ELMs can also be achieved in low ν^* conditions, as shown in Fig. 2 (red points from JET and light-green from JT-60U), in which the previous database of ELM energy losses is overlaid with the new experimental results from JET [7] and JT-60U [8]. It is important to note, however, that the plasma conditions which are required to access this ELM regime are not compatible with the requirements for $Q_{DT} = 10$ operation in ITER, either

because of the need for high q_{95} (~ 4.5) or the strong deterioration of plasma energy confinement as density is increased to achieve $\langle n_e \rangle$ ~ 0.85 n_{GW}. Experiments are in progress to understand the interplay between the achievement of convective ELMs, global energy confinement and accessibility to high densities in order to bring these regimes closer to ITER's requirements.

The ELM energy lost from the main plasma is deposited onto the main wall and divertor PFCs targets in present devices within timescales and with spatial distributions which are determined by the transport of plasma energy via the electron and ion channels as described in [10] for JET, consistent with MAST [11] and ASDEX Upgrade [12] observations. ELMs lead to the expulsion of energy in the outer region of the device, part of which is contained in so-called filaments, which are not toroidally symmetric plasma structures aligned to the magnetic field. The role of the dynamics of these filaments on the
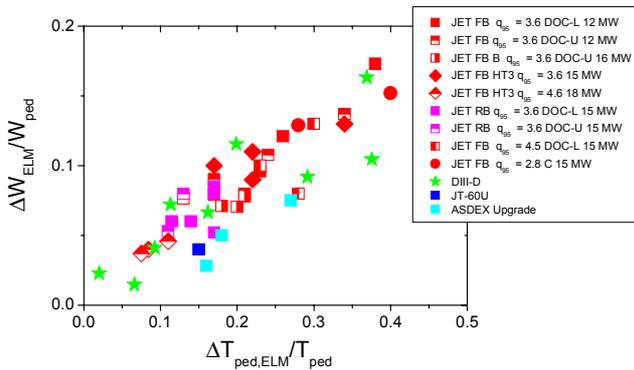

Figure 1. Normalised ELM energy drop versus normalised ELM temperature drop for a range of JET (low/high triangularity, q_{95} = 2.8 - 4.5 and forward and reversed field), DIII-D, JT-60U and ASDEX-Upgrade Type I ELMy H-modes showing the correlation between small ELM energy losses and convective ELMs (small temperature drop).
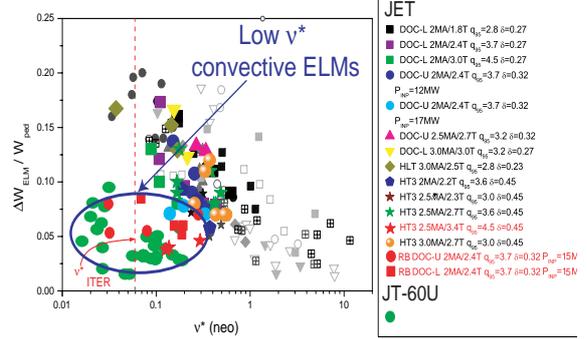
Fig. 2. Normalized ELM energy loss ($\Delta W_{ELM}/W_{ped}$) vs. pedestal collisionality (ν^*) for Type I ELMy H-mode plasmas (grey) and newer results from JET/JT-60U. The JET data includes a range of I_p plasma shapes, q_{95} and two directions of B_ϕ. Low ν^* convective ELMs are shown in red for JET.

power deposition on PFCs in experimental devices is subject of active research but some features are common to all results obtained until present : a) Despite a possible non-toroidal symmetry of the ELM energy outflux, the magnetic field properties near the X-point and the associated enhanced diffusion, together with the toroidal rotation of the filaments lead to a toroidally symmetric power deposition profile at the divertor target during ELMs, in a region corresponding to 1-1.5 cm at the outer midplane [13] with a footprint similar to that between ELMs. b) The timescale for the ELM divertor power flux rise is correlated with the parallel ion transport timescale leading to an expected power flux rise time for ITER in the region of 250-500 μs. During this time interval typically less than 30% of the total ELM divertor energy flux reaches the divertor target [7, 14], the remaining arriving in a time interval typically three times longer than that of the power rise time, as shown in Fig. 3. These observations are in agreement with a model recently developed to describe the radial and parallel flux of energy during transients in the SOL of tokamaks which describes satisfactorily JET measurements [10, 15, 16]. c) The flow of ELM energy onto main chamber PFCs is dominated by convection of energy via the ion channel associated with the fast radial propagation of plasma originating from the confined plasma during the ELMs. Typical radial propagation velocities of the particles expelled during ELMs are in the range of 0.5-1 kms^{-1} [11, 12, 15], which are typically $v_{ELM}/c_{s,ped}$ = 0.5-3 10^{-3}, where v_{ELM} is the average radial speed for ELM particle propagation and $c_{s,ped}$ is the sound speed calculated with plasma parameters at the pedestal. The scaling of the radial velocity with pedestal

plasma parameters is present subject of research. Experiments in DIII-D [17] show a large dependence of the scale length of the density profile near the separatrix (λ_n) with ELM energy loss, as shown in Fig. 4 (in terms of the derived v_{ELM} from the measured λ_n by $\lambda_n = v_{ELM} L / c_{s,ped}$, where L is the SOL connection length), with $v_{ELM} \sim (\Delta W_{ELM}/W_{ped})^{0.7-2.0}$. These dependencies are somewhat stronger than that proposed recently $v_{ELM}/c_{s,ped} \sim (\Delta W_{ELM}/W_{ped})^{0.5}$ [18], which is consistent with the deficit of energy found at the divertor for large ELMs at JET [14] and are, thus, taken as an upper bound to the expected v_{ELM} in ITER.

Assuming that for ITER v_{ELM} is within the range seen in present experiments, the amount of energy which can flow to the various PFCs in ITER for typical pedestal-separatrix conditions is estimated by the model in [10, 15], as shown in Fig. 5.a and Fig. 5.b, for a range of assumptions with respect to the poloidal extent and other ELM characteristics in ITER, parallel and perpendicular transport and sheath physics during transients (see [15] for details). For large v_{ELM}, the proportion of ELM energy that reaches PFCs outside the divertor can be significant (more than 20% of ΔW_{ELM}) and, correspondingly, the associated parallel fluxes are in the range of several GWm^{-2}.
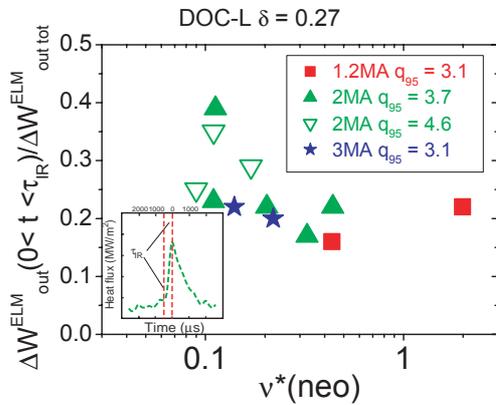

Fig.3 Proportion of the ELM energy arriving at the divertor in the time interval $[0, \tau_{IR}]$ (i.e. ELM start to the time of maximum power flux as shown in the inset) with respect to the total ELM divertor energy versus pedestal collisionality for a range of Type I ELMy H-modes at JET.
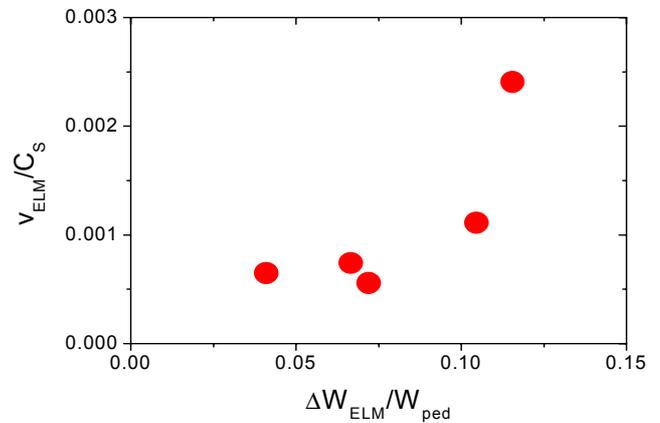

Fig. 4. Derived ELM radial propagation velocity versus normalised (versus pedestal energy) ELM energy loss from DIIID measurements [17].

3. Power fluxes at the ITER plasma edge during disruptions

Disruptions in ITER have the potential to produce the largest energy fluxes and PFC damage as, contrary to ELMs which only lead to a decrease of $\sim$ 3-10% of W_{plasma}, the whole energy of the plasma can be lost to PFCs during the thermal quench. In practice, by the time the discharge reaches the thermal quench, the plasma energy confinement has been severely deteriorated and, on-average, the plasma energy is less than 50% of that as full performance, as shown in Fig. 6 for JET and ASDEX-Upgrade [2, 19]. It is not clear at present if the lower plasma energy measured at JET is due to a favourable size scaling or to disruption amelioration actions, which are applied routinely at JET but not in ASDEX-Upgrade. As a consequence of this pre-disruption decrease of τ_E, increased power fluxes (to the divertor mostly) are measured in advance of the disruption thermal quench. In general, the timescale of these fluxes is longer than the energy confinement time and, thus, they are of low magnitude compared to those at the thermal quench. Only when fast phenomena are involved, such as a growth of MHD modes and locking and fast H-L transitions, as shown in Fig. 7 for JET, can the pre-disruptive divertor power fluxes be significant compared to the thermal quench. This is, in part, due to the lack of a significant broadening of the power flux footprint during these transitions, contrary to the

observations during the thermal quench [20]. In such fast transients the plasma can deposit an amount of energy in the range of 10-50% of that at full performance in timescales typically a factor of 5-10 smaller than the full-performance τ_E, as seen in JET and MAST. On the basis of these measurements, pre-disruptive fast transients in ITER could lead to power pulses of magnitude/duration in the range ~ 14 MWm^{-2}/0.72 s to 140 MWm^{-2}/0.36 s at the divertor target. Only for the occasional disruption that leads to power fluxes in the upper range of the values above, the pre-disruptive power fluxes can cause significant erosion of the divertor target by the surface temperature reaching the sublimation (CFC) or melting temperature (W).
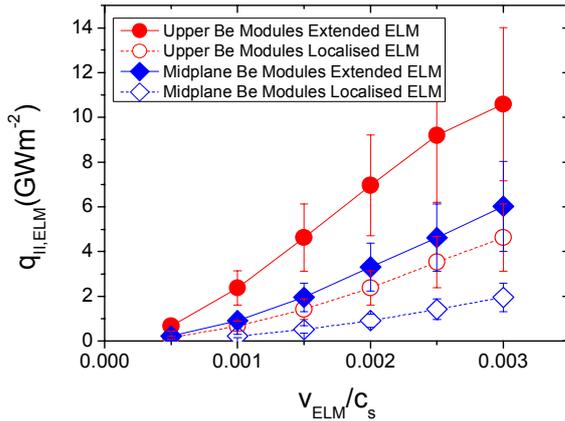

Fig. 5.a. ITER peak ELM energy fluxes along B at the upper X-point Be modules (5 cm from separatrix) and at the outer midplane Be limiter (10 cm from separatrix) for a range of ELM radial velocities and assumptions on ELM poloidal extent (localised at the outer midplane or extended in the outer side of the plasma)
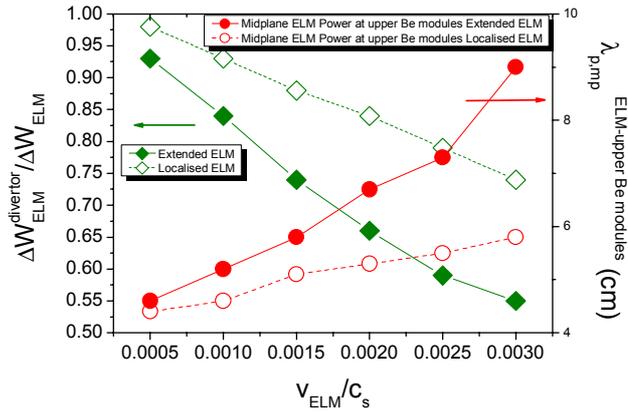
Fig. 5.b. Proportion of the ELM energy released from the main plasma which reaches the divertor target in ITER for the same assumptions as in Fig. 5.a and decay length of the parallel flux (mapped to the midplane) for the SOL lines intersecting the upper X-point Be modules.

It is, thus, of highest importance for the estimation of PFC lifetime in ITER to determine the magnitude and spatial/temporal characteristics of the power fluxes during the thermal quench of disruptions. Present experimental results, in agreement with the basic findings summarised in [3] show that : a) During the thermal quench the power footprint at the divertor is significantly broadened (by a factor of 5-10) with respect to that during the full performance phase and, thus, a significant amount of the plasma energy flux reaches PFCs outside the divertor region, b) The expected duration of the power rise time of the thermal quench in ITER is in the range of 1-3 ms due to the positive size scaling of this time, although the variation of this timescale within every device can be up to a factor of 5, c) Similar to ELMs, a significant amount of power arrives at the divertor during the decay phase of the thermal quench power pulse, which is typically a factor of 2-3 longer than the rise time and, thus, only ~ 30% of the total divertor energy flux during the thermal quench reaches the target within the rise time phase [21].

Taking into account the above experimental findings and assuming that they are applicable to ITER, it is possible to evaluate the power fluxes expected to reach the PFCs in ITER during the thermal quench for a range of conditions. The typical magnitude of the parallel power flux during the thermal quench of disruptions is the range of 10-100 GWm^{-2} for the separatrix, 3-10 GWm^{-2} for the field line intersecting the upper X-point Be modules and 1-3 GWm^{-2} for the field line intersecting the limiter.

4. Power fluxes onto ITER PFCs during Type I ELMs and disruptions and associated erosion

The actual fluxes reaching the various PFCs in ITER depend not only on the fluxes along the field evaluated above but also on the geometry of the magnetic field and that of PFCs themselves. In first place, from the results in Fig, 5.b and assuming no significant broadening of the divertor power footprint during ELMs (i.e., a divertor effective area of 3.5 m^2) and an ELM power rise time of 375 µs, the peak ELM power flux at the divertor can be derived. The estimate of the power fluxes during ELMs on the first wall is more complex. In fact, the lack of a complete model for the description of the transport of energy from the confined plasma to the PFCs leads to two possible ways to extrapolate the results in Figs. 5.a and 5.b to ITER. In the first approach, one can simply take the calculated power fluxes along the field in Fig. 5.a and project them onto the upper X-point Be modules on which the typical incidence angle is less than 1°, given the proximity of the upper X-point to the Be wall in ITER (these results are shown in Fig. 8.a). Alternatively, the global results in Fig. 5.b can be applied by evaluating the effective area of the upper X-point region for power deposition on the basis of the calculated λ_q in Fig. 5.b and the corresponding flux expansion (~ 25) (these results are shown in Fig. 8.b). The differences between the estimated power fluxes by both approaches is a factor of ~ 2, which is expected given the assumptions required to derive the fluxes by the two approaches.
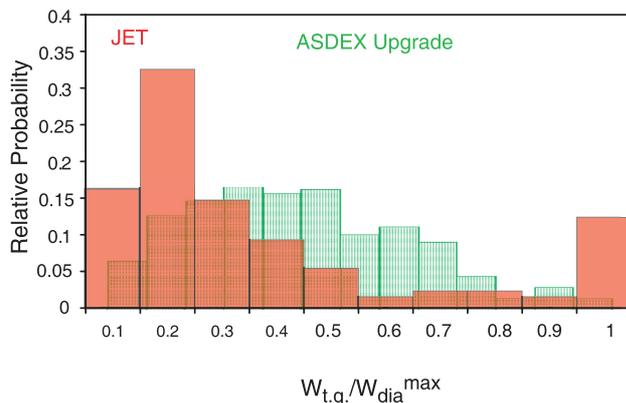

Figure 6. Relative probability for the fraction of disruption thermal energy in JET and ASDEX-Upgrade for a database of high energy disruptive discharges.
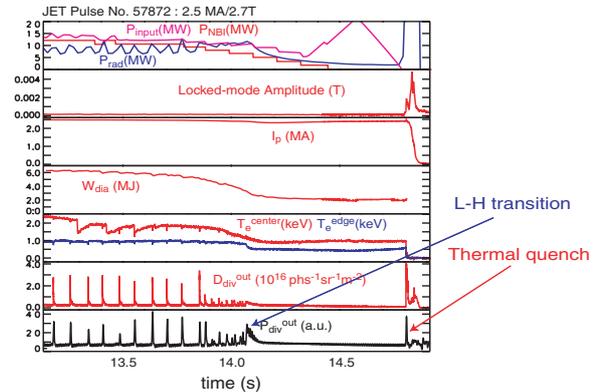

Figure 7. Plasma parameters in the approach to a disruption following a L-H transition at JET showing the transient power flux at the divertor during the transition and the thermal quench.

According to these results even the largest ELMs in ITER would be not lead to melting of the upper X-point Be wall modules. The corresponding "ablation-melting" parameters would be ~ 10 MJm^{-2}s$^{-1/2}$, which lower than that required for melting of Be ~ 16 MJm^{-2}s$^{-1/2}$. It is important to note, however, that this relies on the effective use of the whole available area of the upper X-point modules for distributing the ELM power pulse (more than 50 m^{-2}) uniformly toroidally. Two major issues have to be taken into account in this respect : a) For the low angles of incidence expected in this region ($\sim 1^o$ and lower) the required alignment of the blanket modules to achieve this toroidal uniformity in ITER maybe very challenging and b) ELM power fluxes for field lines at a distance larger than 1-1.5 cm at the outer midplane are likely to be very toroidally non-uniform increasing considerably the local ELM power flux over the toroidal averages calculated above. With these caveats, one can foresee that the operation of ITER with ELM energy loads that lead to an acceptable divertor lifetime is, thus, likely to be acceptable for the main Be wall (at least for the upper X-point Be modules).

In a similar way, disruption energy fluxes at ITER PFCs can be derived from the parallel fluxes. In this case the typical power fluxes at the divertor are several GW m^{-2} and

500 MWm^{-2} at the upper Be modules (assuming toroidal uniformity) with a duration in the range of 1.5-3.0 ms for the upper range of plasma energies at the thermal quench. For such conditions, significant CFC sublimation at the divertor and Be melting/evaporation at the upper blanket modules can occur. For disruptions in which the energy confinement is strongly deteriorated before the thermal quench this can be avoided.

Utilising the results above and taking into account that a reasonable description of the experimentally measured temporal dependence of ELM and disruption transient loads is given by [15] $q(t) = (1+(t/\tau)^2)(t/\tau)^2 e^{-(t/\tau)^2}$, where τ is related to the characteristic rise time determined experimentally, it is possible to determine the expected material erosion at the divertor and main wall for the power fluxes derived above, as shown in Fig. 9.a and 9.b. From these results, it is clear that repetitive ELM loads at the ITER divertor should be maintained below 1 MJm^{-2} for an acceptable divertor lifetime, which is equivalent to a total divertor ELM energy flux of 3.5 MJ. This corresponds to $\Delta W_{ELM}/W_{ped} < 5 \%$, $v_{ELM}/c_{s,ped} \sim 5 \times 10^{-4}$ and $\Delta W_{ELMdiv}/\Delta W_{ELM} > 92\%$, which can only be achieved if convective ELMs are obtained for the ITER reference scenario. The expected loads on the upper Be modules are less than 0.2 MJm^{-2}, which will not cause Be melting. For disruptions, the maximum energy load for acceptable divertor lifetime has to remain under 6 MJm^{-2}. This is equivalent to a total plasma energy at the time of disruption of 105-210 MJ, which is well within the expectations of the energy confinement degradation in the pre-disruption phase shown in Fig. 6. For these conditions the expected loads on the upper Be modules are in the range 0.4-1.0 MJm^{-2}, which are lower but close to those required to cause significant Be melting of these modules.

5. Conclusions

Progress in experimental research on ELMs and disruption loads in present tokamaks has allowed refining the extrapolations of these loads to ITER. Operation of ITER with convective Type I ELMs in the reference scenario is required to maintain a sufficient lifetime of the divertor targets. If this is achieved, the loads on the main wall are not expected to cause significant erosion of the Be-clad blanket modules by ELMs. For disruptions, the divertor lifetime is probably satisfactory for the expected $\sim$ 10% full-performance plasma disruption frequency, when the pre-disruption energy confinement degradation and power flux broadening during the thermal quench are taken into account. The lifetime of the Be-clad blanket modules is more difficult to determine due to the proximity to melting in these events but, unless a large proportion of the disruptions occur at the high energy range, this should be restricted to a relatively small number of disruptions leading to an adequate Be lifetime for disruptions as well. It is important to point out that, in these estimates, the PFC loads are assumed to have a large degree of toroidal symmetry and that erosion to materials is estimated with their average properties. Recent experiments in dedicated facilities and modelling have shown that the erosion of real materials/components can deviate significantly from this idealised estimates with the corresponding implications for the maximum loads which are expected to be acceptable in ITER [4, 5].

6. References

[1] Rapp, J. et al., Nucl. Fusion **44** (2004) 312.
[2] Federici, G., et al, Plasma Phys. Control. Fusion **45** (2003) 1523.
[3] Loarte, A., et al., Proc. 20th IAEA Conference, 2004 Vilamoura Portugal.
[4] Zhitlukhin, et al., 17th PSI Conference, Hefei, China, 2006.
[5] Linke, J., et al., this conference.
[6] Leonard, A., et al., et al, Plasma Phys. Control. Fusion **44** (2002) 945
[7] Loarte, A., et al., Phys. Plasmas **11** (2004) 2268.

[8] Oyama, N. et al., Nucl. Fusion **45** (2005) 871.

[9] Urano, et al., et al, Plasma Phys. Control. Fusion **46** (2004) A315.

[10] Pitts, R.A., et al., this conference.

[11] Kirk, A., et al., Plasma Phys. Control. Fusion **47** (2005) 315.

[12] Herrmann, A., et al., Plasma Phys. Control. Fusion **46** (2004) 971.

[13] Eich, T., et al., Phys. Rev. Lett. **9119** (2003) 5003.

[14] Eich, T., et al., Jour. Nuc. Mat. **337-339** (2005) 669

[15] Fundamenski, W., et al., Plasma Phys. Control. Fusion **48** (2006) 109.

[16] Eich, T., et al., 17th PSI Conference, Hefei, China, 2006.

[17] Zeng, L., et al., Plasma Phys. Control. Fusion **46** (2004) A121.

[18] Fundamenski, W., et al., 17th PSI Conference, Hefei, China, 2006.

[19] Riccardo, V. et al., Nucl. Fusion **45** (2005) 1427

[20] Counsell, G., et al. Proc. 2004 EPS Conference, London, UK.

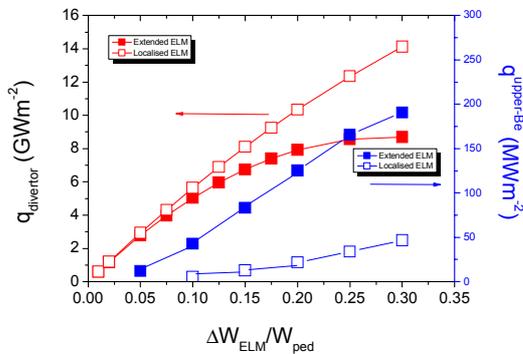[21] Pautasso, G., et al., Proc. 2004 EPS Conference, London, UK.

Figure 8.a. ELM power flux at the divertor and the upper X-point Be modules. The value of the power flux at the upper X-point Be modules is derived from the parallel power fluxes in Fig. 5.a.
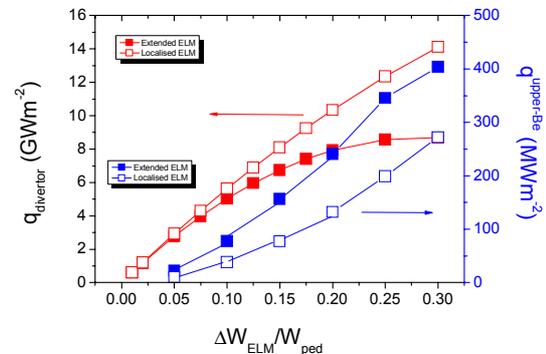

Figure 8.b. ELM power flux at the divertor and the upper X-point Be modules. The value of the power flux at the upper X-point Be modules is derived from the global energy balance and the ELM power decay lengths in Fig. 5.b
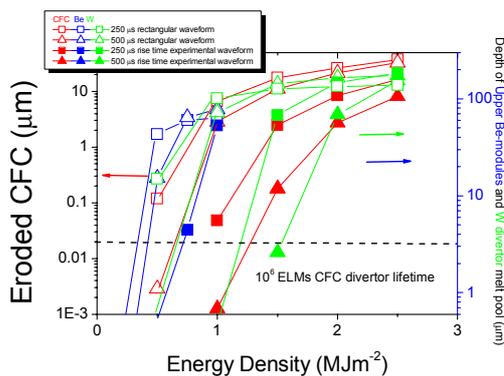

Figure 9.a. Estimated CFC erosion and W/Be melt pool depth for a range of energy loads and timescales typical of ELM power fluxes at the divertor and at the upper X-point Be modules in ITER.
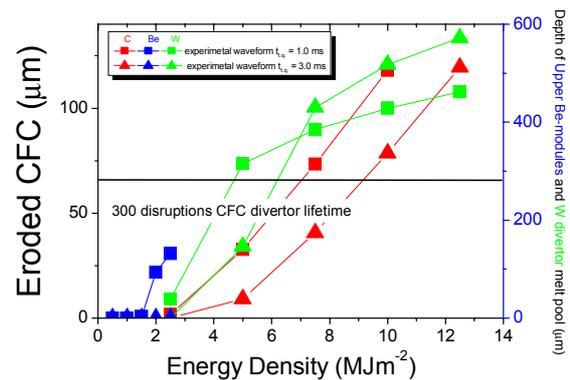

Figure 9.b. Estimated CFC erosion and W/Be melt pool depth for a range of energy loads and timescales typical of disruption thermal quench power fluxes at the divertor and at the upper X-point Be modules in ITER.